POLITECNICO DI TORINO
Repository ISTITUZIONALE

Aerodatabase Development and Integration and Mission Analysis of a Mach 2 Supersonic Civil Aircraft

(Article begins on next page)

19 September 2024

Article

Aerodatabase Development and Integration and Mission Analysis of a Mach 2 Supersonic Civil Aircraft

Pietro Roncioni [1,*], Marco Marini [2], Oscar Gori [3], Roberta Fusaro [3] and Nicole Viola [3]

1 Aerothermodynamics Department, Centro Italiano Ricerche Aerospaziali, 81043 Capua, Italy
2 Technology Integration and System Engineering Department, Centro Italiano Ricerche Aerospaziali, 81043 Capua, Italy; m.marini@cira.it
3 Mechanical and Aerospace Engineering Department, Politecnico di Torino, 10129 Turin, Italy; oscar.gori@polito.it (O.G.); roberta.fusaro@polito.it (R.F.); nicole.viola@polito.it (N.V.)
* Correspondence: p.roncioni@cira.it

Abstract: The request for faster and greener civil aviation is urging the worldwide scientific community and aerospace industry to develop a new generation of supersonic aircraft, which are expected to be environmentally sustainable and to guarantee a high-level protection of citizens. A key aspect to monitor the potential environmental impact of new configurations is the aerodynamic efficiency and its impact onto the real mission. To pursue this goal, this paper discloses increasing-fidelity aerodynamic modeling approaches to improve the conceptual design of high-speed vehicles. The disclosed methodology foresees the development of aerodynamic aerodatabases by means of incremental steps starting from simplified methods (panels methods and/or low-fidelity CFD simulations) up to very reliable data based on high-fidelity CFD simulations and experimental measurements with associated confidence levels. This multifidelity approach enables the possibility of supporting the aircraft design process at different stages of its design cycle, from the estimation of preliminary aerodynamic coefficients at the beginning of the conceptual design, up to the development of tailored aerodatabases at advanced design phases. For each design stage, a build-up approach is adopted, starting from the investigation of the clean external configuration up to the complete one, including control surfaces' effects and, if any, the effects of the integration of the propulsive effects. In addition, the applicability of the approach is guaranteed for a wide range of supersonic and hypersonic aircraft, and the developed methodology is here applied to the characterization of Mach 2 aircraft configuration, a relevant case study of the H2020 MORE&LESS project.

Keywords: aerodynamic characterization; supersonic civil transport; aerodatabase building; H2020 MORE&LESS project

1. Introduction

The request for faster and greener civil aviation is urging the worldwide scientific community and aerospace industry to develop a new generation of supersonic aircraft, which are expected to be environmentally sustainable and to guarantee a high-level protection of citizens. Thanks to a considerable number of research activities carried out in the last decades, some innovative supersonic aircraft concepts now have the potential to ensure technically viable solutions to fly beyond the speed of sound at higher altitudes with respect to current civil aviation, but no commonly agreed regulations and procedures to support their eventual operations exist. To pursue this purpose, MORE&LESS (**MDO** and **RE**gulations for **L**ow boom and **E**nvironmentally **S**ustainable **S**upersonic aviation), answering to the EC call "Towards global environmental regulation of supersonic aviation" (LC-MG-1-15-2020) [1–5] aims at supporting Europe to shape global environmental regulations for future supersonic aviation: recommendations are established on the basis of the outcomes of extensive high-fidelity modeling activities and test campaigns that merge into the multidisciplinary optimization framework to assess the holistic impact of supersonic

aviation on the environment. To achieve its main goals, the H2020 MORE&LESS project pursues a multifidelity approach in which analytical formulations are tuned thanks to high-fidelity numerical simulations, which are, in turn, validated against experimental test campaigns. This approach is applied to various disciplines in the project, from propulsion [6–9] and combustion [10,11] to aerodynamic [12–18], jet-noise [19] sonic-boom [20], and, eventually, to the environmental assessment [21–23]. This paper specifically focuses on the development of this multifidelity approach to support the aerodynamic characterization of sustainable high-speed aircraft configurations. This paper deals with the development and integration of increasing-fidelity aerodynamic modeling in the conceptual design of supersonic/hypersonic cruisers. This methodology foresees the development of aerodynamic databases by means of incremental steps starting from simplified methods, such as low-fidelity CFD (computational fluid dynamics) simulations, up to very reliable data based on high-fidelity CFD simulations and experimental measurements with associated confidence levels. This multifidelity approach, here disclosed, enables the possibility of supporting the aircraft design process at different stages of its design cycle, from the estimation of preliminary aerodynamic coefficients at the beginning of the conceptual design, up to the development of tailored aerodatabases at advanced design phases. For each design stage, a build-up approach is adopted, starting from the investigation of the clean external configuration up to the complete one, including control surfaces' effects and, if any, the effects of the integration of the propulsive effects. This approach allows a full characterization of forces and moments acting on the vehicle, thus enabling a reliable trajectory analysis. In addition, the applicability of the approach is guaranteed for a wide range of supersonic and hypersonic aircraft, and the developed methodology is here applied to the characterization of Mach 2 aircraft configuration, a relevant case study of the H2020 MORE&LESS project. This paper discloses results of research activities carried out in the H2020 MORE&LESS project. One of the project strengths lies in the possibility of coupling numerical and analytical investigations with experimental test campaigns. However, with the available resources, only few case studies are currently undergoing tests. Specifically, as far as the aerodynamics are concerned, two different Mach 5 configurations will be analyzed in wind tunnels. However, the comparison of the results obtained so far for the Mach 5 configuration can be used as a valuable basis to understand the errors margins characterizing numerical and analytical formulations for other aircraft configurations.

2. State of the Art

After the retirement of the Concorde, both Europe and US diverted their attention on civil flight mainly towards the efficiency improvement. However, in the last few years, in line with the European Commission interests, we are also assisting with the renewed interest in supersonic transport by a few US companies for both business and common routes. In this context, there is flourishing research about aerodynamic investigations of very different aircraft configurations [24–29].

The current and more widely used procedures for a complete and untouched aerodatabase development foresee the execution of both CFD numerical simulations and experimental test campaigns [24]. The double activity is conducted for several purposes: first of all, to have a cross check that can be considered validating for both the sources of data, and, moreover, to build a reliable uncertainties database to be added to nominal values that come from experimental/CFD data. Usually, the experimental test campaigns can provide large amount of data that, once corrected for the WT errors (wall effect, base, sting, etc.) and Reynolds effect (extrapolation to flight), are used as the base for the building of nominal values.

Recently, some deviations from this standard procedure have been used, as the direct use of CFD results in nominal values exploiting the recent high-performance computing (HPC) of modern computer architectures that allow full rapid characterization of the flight envelope [29]. In this case, the experimental data are used to cross check the procedure and to build the uncertainties error bars. In particular, the current paper's procedure is a

very rapid way to obtain an integral database. Is uses a build-up approach putting together inviscid CFD runs, tuned viscous corrections, and control surfaces effects. The results are validated with ad hoc selected viscous CFD simulations and, if available, with experiments.

3. Aerodatabase Building

This section discloses the step-by-step methodology developed in the framework of the H2020 MORE&LESS project. A multifidelity and multidisciplinary approach is followed, where each step of the design phase involves multiple analyses with equal level of details. For the purpose of this paper, the main focus is on the aerodynamic modeling and mission simulation, as shown in Figure 1. The aerodatabase of a generic high-speed civil aircraft considered in the framework of the project is built starting from preliminary aerodynamic data obtained by means of inviscid CFD up to a final and more reliable aerodatabase setup with viscous CFD and experimental measurements and associated confidence level bars. In parallel with the aerodynamic analysis, mission simulation is run at each stage of the design phase, to have a fast and reliable estimation of the vehicle performance along the reference trajectory. The mission simulation, commonly regarded as the ultimate validation of a given concept, is exploited here from the early design phases, guaranteeing accuracy in estimating nominal ranges, fuel mass, fuel reserves, etc., at every stage of the design process.
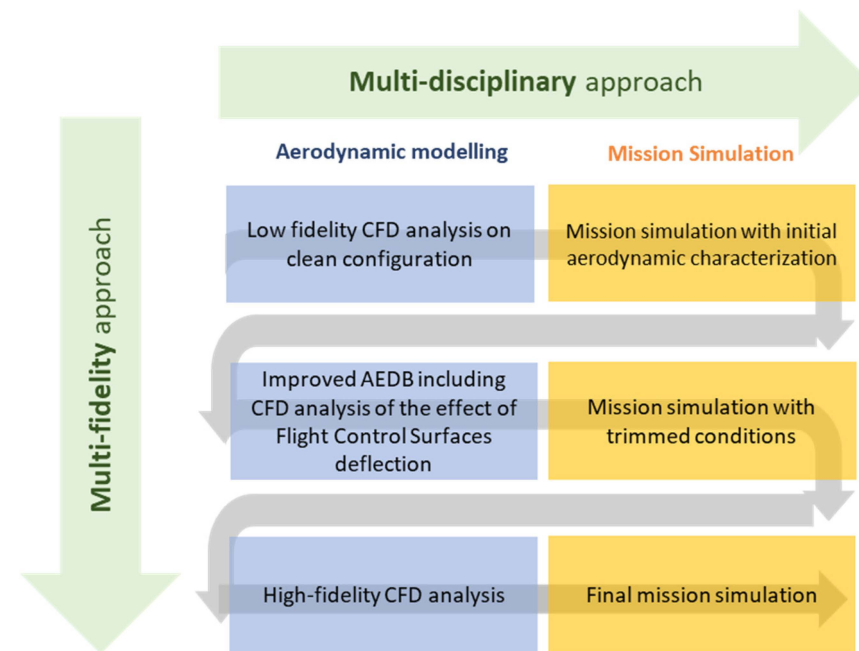
Figure 1. Methodology overview.

3.1. Low-Fidelity Aerodatabase

At the first stage, the aerodynamic modeling consists of the investigation of the clean configuration (with undeflected control surfaces). Based on the experience gained in the H2020 STRATOFLY project (Horizon 2020 STRATOspheric FLYing Opportunities for High-Speed Propulsion Concepts Project), inviscid CFD simulations are used on the clean configuration, and then properly tailored viscous effects corrections are applied [30]. These corrections can be estimated through engineering formulations, which are widely available in the literature and whose coefficients can be tuned to properly capture the peculiarities of the vehicle and its flight trajectory.

It is important noticing that the supersonic/hypersonic panels method (surface impact method tool), based on classical modified-Newtonian, tangent-wedge, and shock-expansion theories, are widely used in these preliminary design stages [31,32]. Even if these theories and tools provide a valuable support for the aerodynamic characterization of high-speed vehicles throughout the supersonic and hypersonic speed regimes, they cannot be used to

predict the behavior of such vehicles along the transonic and subsonic phases. Therefore, inviscid CFD simulations are preferred.

The aerodynamic coefficients, in a wind axis reference frame, are defined as follows:

$$C_L = \frac{L}{\frac{1}{2}\rho V^2 S_{ref}}; C_D = \frac{D}{\frac{1}{2}\rho V^2 S_{ref}}; C_{My} = \frac{M_y}{\frac{1}{2}\rho V^2 S_{ref} L_{ref}}$$

where C_L is lift coefficient, C_D is drag coefficient, C_{My} is pitching moment coefficient, L is lift force, D is drag force, M_y is pitching moment (around y axis), ρ is density, V is velocity, S_{ref} is reference surface area, and L_{ref} is reference length.

Once the clean configuration is available, properly tailored viscous effects corrections can be applied. Based on what is available in the literature, the viscous effect engineering formulation can be generalized as follows:

$$(\Delta C_D)_{visc} = \alpha * \frac{1}{\left[Log\,(Re)\right]^{2.58}} * \frac{1}{(1 + \beta * M^2)^{\gamma}} * \frac{A_{wet}}{A_{ref}}, \tag{1}$$

where the viscous contribution to the drag ($(\Delta C_D)_{visc}$) can be estimated by correcting the turbulent flat plate theory (represented by the term $\frac{1}{\left[Log\,(Re)\right]^{2.58}}$; see [33,34], where Re is the Reynolds number) with (i) the factor $\frac{1}{(1+\beta*M^2)^{\gamma}}$ (M: Mach number) which takes into account the compressibility effect, and with (ii) the wetted-to-reference area ratio. The parameters α, β, and γ can be customized depending on the vehicle configuration. For example, the values $\alpha = 0.43$, $\beta = 0.31$, and $\gamma = 0.37$ were found for the STRATOFLY MR3 configuration [30]. Moreover, a preliminary direct comparison of the results of the previous formulations with both viscous CFD and experimental measurements can be found in Figure 2, where the drag coefficient of another vehicle of the MORE&LESS project (CS2 of Figure 3) is reported (less than 7% difference).
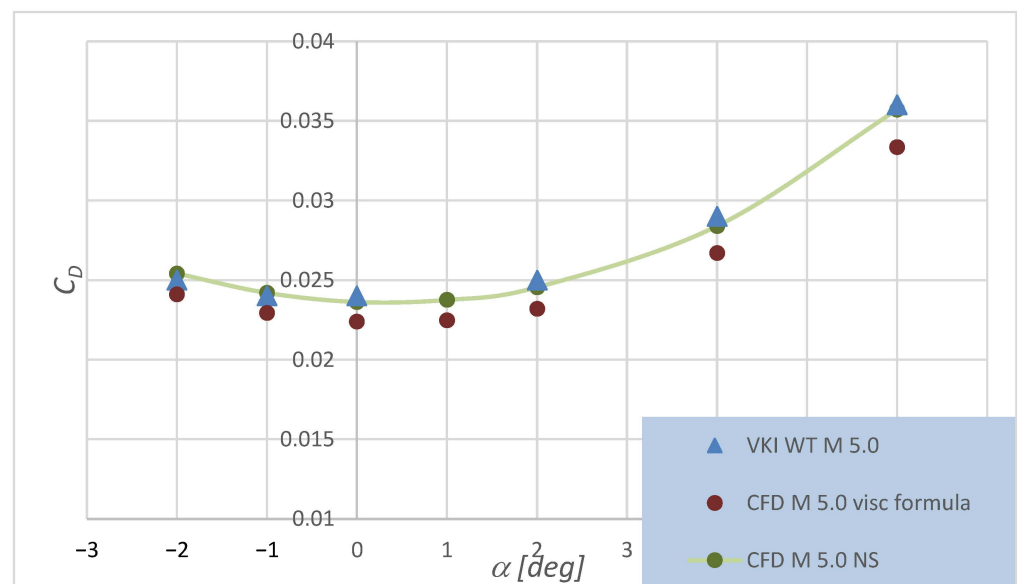

Figure 2. Drag coefficient at Mach 5 of VKI WT CS2 vehicle. Comparison between WT data (1st line of legend), inviscid CFD with viscous correction (2nd line of legend), and direct viscous CFD (3rd line of legend).

The general formulation is synthesized in the following formulation (for the longitudinal flight and body axis reference frame), where the nominal coefficients (C_N, C_A, C_{My}) (C_N: normal force, C_A: axial force) are obtained as a sum of several contributions: clean

configuration, the sum of effects of each control surfaces deflection, viscous effects, and thrust contribution:

$$C_N = (C_N)_{clean} + \sum_{surf=1}^{n} (\Delta C_N)_{surf}$$

$$C_A = (C_A)_{clean} + (\Delta C_A)_{visc} + \sum_{surf=1}^{n} (\Delta C_A)_{surf} \qquad (2)$$

$$C_{My} = (C_{My})_{clean} + \sum_{surf=1}^{n} (\Delta C_{My})_{surf} + (\Delta C_{My})_{Thrust}$$

where subscripts are as follows: clean for clean configuration, *surf*: control surface deflection, Thrust for engine thrust contribution, and *n* for total number of control surfaces.
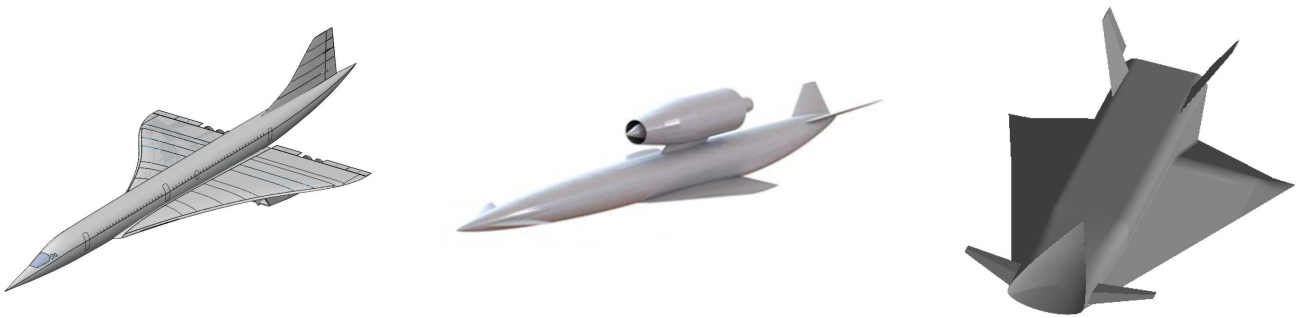
Figure 3. Some of the configurations to be analyzed. CS1 (**left**), CS2 (**center**), CS3 (**right**).

3.2. High-Fidelity Aerodatabase

After preliminary studies, a more reliable aerodatabase is needed in order to refine the design of the aircraft and related mission. The high-fidelity aerodatabase (AEDB) is based on viscous CFD computations and experimental measurements.

The final set of data provides the nominal aerodynamic coefficients, including an appropriate uncertainty level [35]. If case test campaigns are foreseen, the experimental results are used as reference values and uncertainty levels are estimated against them. Conversely, when no experimental data are available, high-fidelity simulations can be used as benchmarks to estimate the uncertainty levels of low-fidelity data. Thanks to this approach, each aerodynamic database, based on the space-based approach (aerodynamics as function of flight conditions and vehicle's attitude and configuration) and build-up formulation, is complemented by a proper uncertainty model.

Two different contributions to uncertainties are considered.

- Tolerances, which represent the confidence level on the aerodynamic coefficients in nominal conditions, and are mainly related to the accuracy of numerical and physical modeling used for the computations (grid, turbulence modeling, etc.) and the quality and accuracy of the experimental data (balance, pressure sensors, repeatability, etc.).
- Variations, which depend on the estimated possible differences between nominal and real flight conditions (both numerical and experimental), and are mainly based on the experience made in previous flights.

Typically, as variations are difficult to estimate in the absence of previous flights, an uncertainty model contains only the tolerances, and the variations are replaced with a safety factor applied on top of the tolerances (i.e., 10%).

The final generic coefficient can be written as the sum of the nominal value and the uncertainty level as follows:

$$C_i\left(M, Re, \alpha, \beta, \delta_{flap}, \delta_{canard}, \delta_{bodyflap}, \delta_{rudder} \right) = C_{i_{nom}} \pm \Delta C_{i,unc} \qquad (3)$$

The above-reported equation is a general representation of a generic aerodynamic coefficient (C_i) as a summation of a nominal value (subscript nom) and a variation (Δ) due

to the uncertainty (subscript unc), where *M* is the Mach number, *Re* is the Reynolds number, *α* is the angle of attack, *β* is the angle of sideslip, and *δ* is the angle of deflection for several control surfaces (flap, canard, bodyflap, rudder, etc.).

3.3. Stability and Trim Analysis

Upon establishing a preliminary layout for the control surfaces, attention must shift towards selecting deflections to ensure that trim conditions are maintained throughout the mission, thereby minimizing adverse effects on the overall efficiency of the vehicle. For a given Mach number and position of the center of gravity, the different control surface deflections are taken into account to analyze the aircraft stability and trim. First, the aircraft stability is verified, checking if the slope of the pitching moment curve, as a function of the angle of attack C_{My_α}, is lower than zero. Then, the trim conditions are computed, imposing $C_{My} = 0$.

3.4. Mission Simulation

Mission simulation [36,37] is run at the end of each iteration, considering the highest-fidelity aerodynamic data available at each design step. The software ASTOS (release 9.17), by Astos Solutions GmbH (Stuttgart, Germany), is used to perform the simulations. The range requirement is set at 6500 km in order to be able to cover a transatlantic mission between Europe and North America. The aerodynamic database is one of the main inputs, together with the vehicle geometric data and the propulsive database.

4. Aerodatabase Building for CS-1

4.1. Case Study

In Figure 3, the reader can find some of the configurations to be analyzed in the framework of the MORE&LESS project. On the left is a Mach 2 "Concorde-like" with biofuel as propellant (CS1, Case Study 1), in the center is an experimental Mach 5 Hypersonic Test Bed (HTB) by Reaction Engines Ltd. (CS2, Case Study 2), and on the right is a Mach 5 scramjet civil aircraft derived from the Mach 8 Stratofly vehicle (CS3, Case Study 3), where the last two are fueled with liquid hydrogen. In this paper, the first configuration, the "Concorde-like" CS1, is considered the general procedure similar for all the vehicles. For the vehicle CS1, the experimental activities are not foreseen and the aerodynamic data are only based on CFD simulations.

The CS-1 vehicle (Figure 4) is a Concorde-like commercial Mach 2 aircraft very similar to the well-known, out-of-service Aérospatiale-BAC Concorde. The main geometrical quantities are the same; in particular, a total length of 62.3 m, a wing span of 25.60 m, and the following reference quantities: S_{ref} = 332.6 m^2; L_{ref} = 27.66 m.
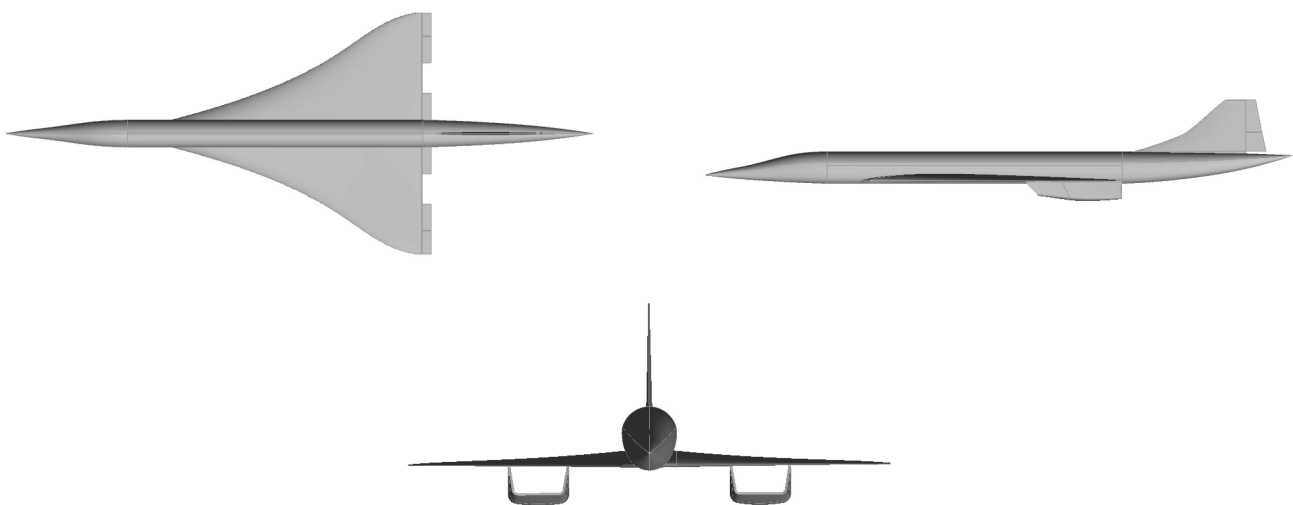

Figure 4. CS1 vehicle three view.

4.2. Aerodatabase Development

Several activities were performed for the development of the present vehicle aerodatabase. A wide range of Mach numbers and angles of attack was considered in order to obtain a complete aerodatabase for the clean configuration and a suitable number of flap deflections, and to study the trimmability and flyability for all flight conditions. In the following is the starting test matrix (Table 1).

Table 1. Test matrix for clean and deflected configurations.

Mach [-]	Clean α [deg]	Flap ($\alpha = 0°$) δ [deg]
0.30	$-5° \to 30°$, step 5°	$-25° \to 25°$, step 10°
0.60	$-5° \to 30°$, step 5°	$-25° \to 25°$, step 10°
0.80	$-5° \to 30°$, step 5°	$-25° \to 25°$, step 10°
0.95	$-5° \to 30°$, step 5°	$-25° \to 25°$, step 10°
1.05	$-5° \to 30°$, step 5°	$-25° \to 25°$, step 10°
1.20	$-5° \to 30°$, step 5°	$-25° \to 25°$, step 10°
1.60	$-5° \to 30°$, step 5°	$-25° \to 25°$, step 10°
2.00	$-5° \to 30°$, step 5°	$-25° \to 25°$, step 10°

The clean configuration low-fidelity data were obtained using an unstructured grid of 2.1 million of cells for half-configuration (longitudinal analysis) generated by means of the ANSYS-ICEMCFD-TETRA® grid generator (Figure 5) and the use of the commercial code Ansys Fluent®. The Euler equations (mass and momentum balances without viscous contributions) were numerically resolved and coupled with a compressible perfect gas state model to close the full system of equations. The following boundary conditions were applied: wall: slip for velocity (null normal component), adiabatic for thermal treatment; and classical far-field conditions for other surfaces of the CFD domain. Particular attention must be given to the modeling of the engine boundary conditions; in particular, the internal flow path of the nacelle was not calculated and the interaction is managed by means of applying the surfaces that act as outflow and inflow for the CFD control volume (Figure 6).
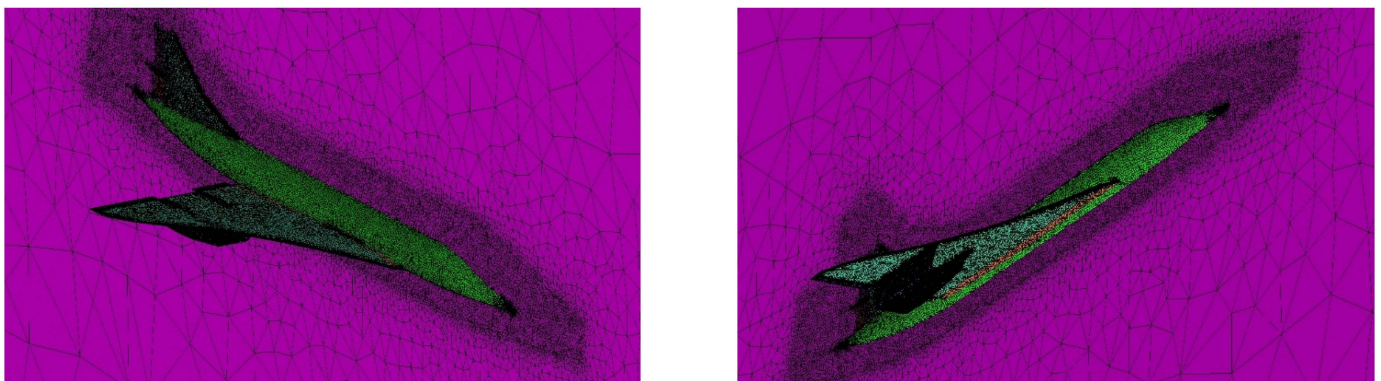
Figure 5. Unstructured grid for CS1 vehicle. Cells 2.1 M.

From Figures 7–9, where all predicted aerodynamic coefficients are reported, a different behavior can be observed for subsonic and supersonic regimes. In particular, the stall phenomenon starts at an angle of attack of 25° in the subsonic regime, whereas for the supersonic one, a quasi-linear trend seems to continue for higher angles of attack.
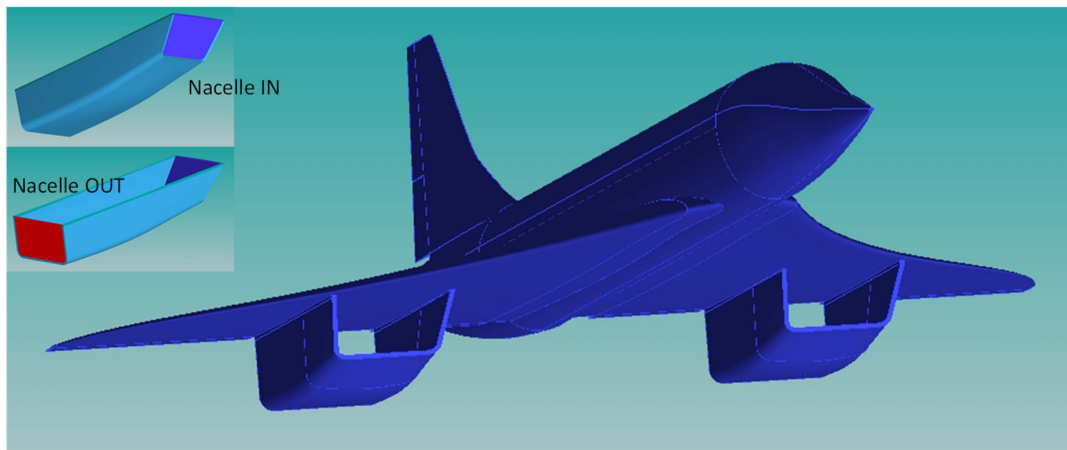
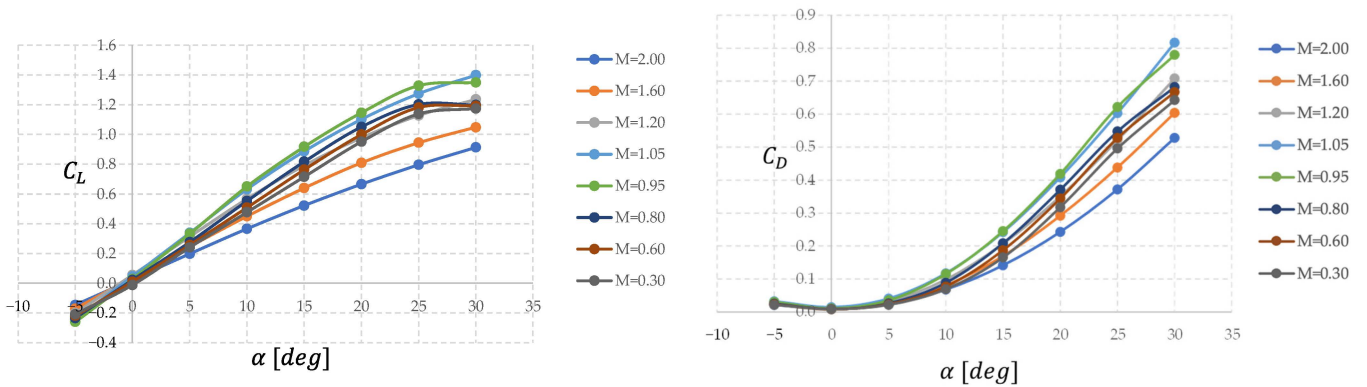**Figure 6.** Global view of the vehicle and boundary conditions treatment.

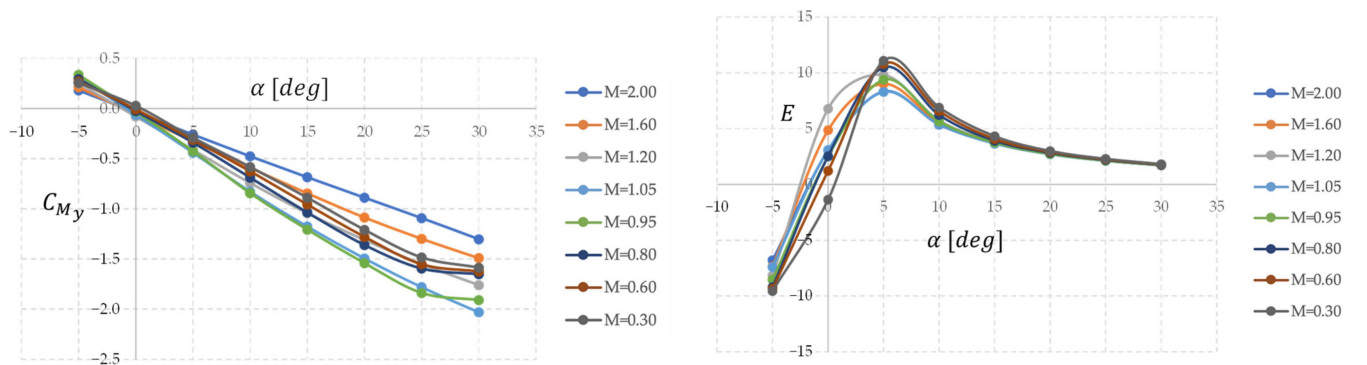**Figure 7.** Lift and drag versus angle of attack for all Mach numbers.

Figure 8. Pitching moments and aerodynamic efficiency versus angle of attack for all Mach numbers.

The trim can be obtained by acting on three different control surfaces as reported in Figure 10. A simplified approach was followed to characterize the control surfaces and reduce the amount of CFD calculations. A standalone wing configuration was considered with several flap deflections (Figure 10). A quasi-linear trend can be found for Delta_CL and a quadratic one for the Delta_CD versus flap deflection (Figure 11). The range of trimmability for a center of gravity located at 50% of the total aircraft's length can observed in Figure 12; it reduces going from lower to higher Mach numbers. This is due to the fact that the center of pressure retreats toward the tail (Figure 13), thus making the trimmability (higher flap deflection to obtain the same angle of attack) harder. The trend of flap deflection versus the desired trimmed angle of attack is reported in Figure 14 for two different center of gravity (CoG) locations (31 and 33 m, i.e., 50% and 53% of total length), where the

reduced trimmability range is confirmed at higher Mach number (Figure 14, left). This behavior at the supersonic regime can be alleviated by shifting the center of gravity toward the tail as it happens for the center of pressure (Figure 14, right). A variable center of gravity along the trajectory seems to be necessary. This behavior is clearer in Figure 15, where the angle of attack of trim is reported versus the Mach number at several flap deflections. A drastic reduction of possible angle of attack can be seen for a center of gravity at 50% of the length (Figure 15, left). The shift of CoG at 53% (Figure 13, right) slightly enlarges the transonic–supersonic region but makes the subsonic regime unstable (the range of trim is outside the figure).
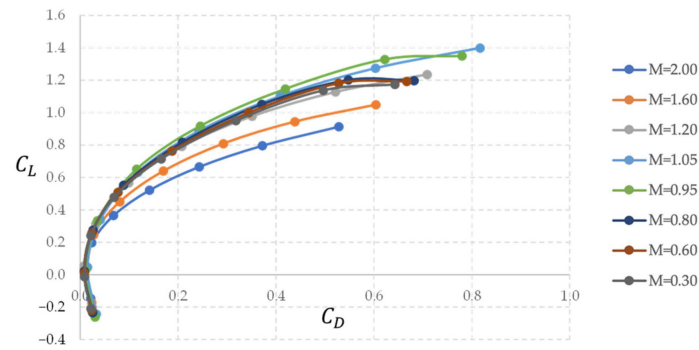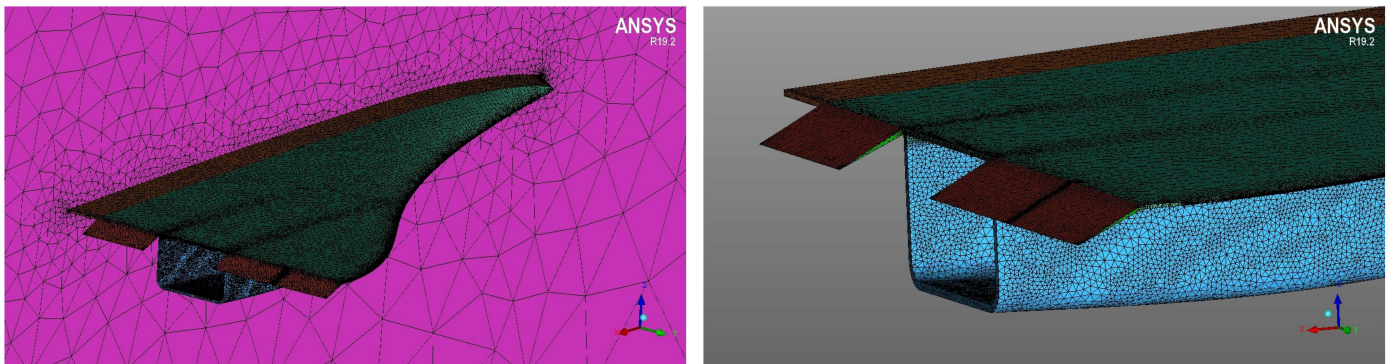

Figure 9. Polars for all Mach numbers.
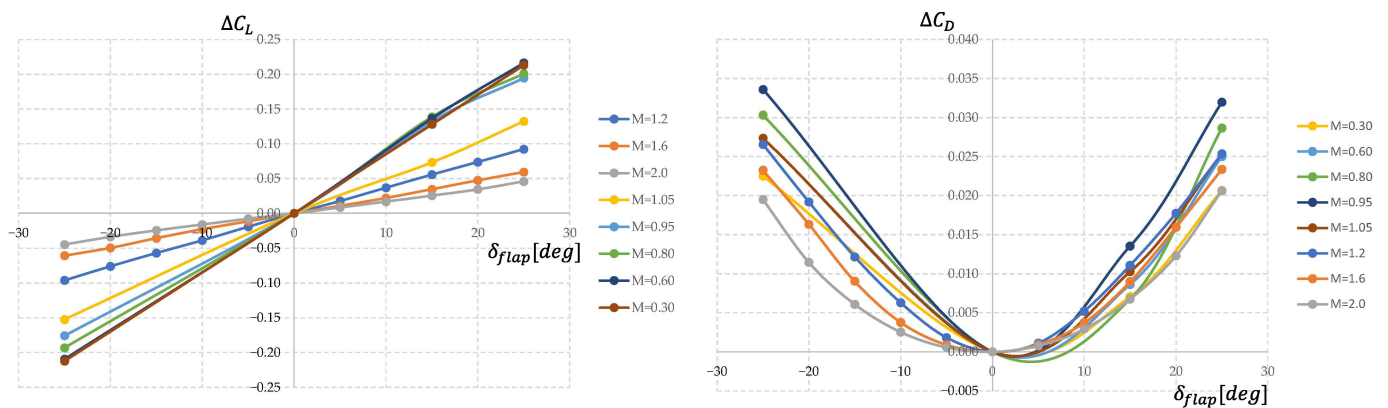

Figure 10. Control surfaces.

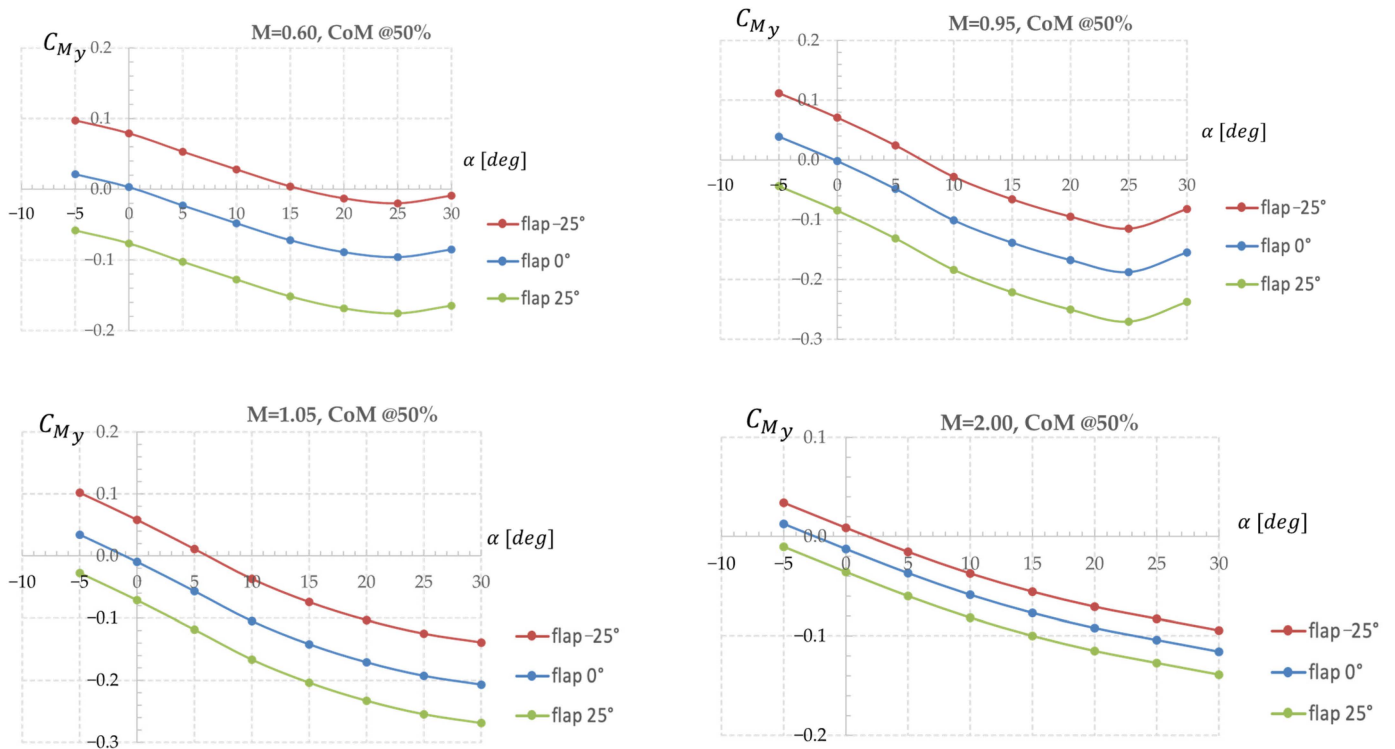**Figure 11.** Effect of control surfaces on lift and drag coefficients versus the flap deflection.

Figure 12. Effect of control surfaces on pitching moment coefficient vs. angle of attack for various Mach numbers.
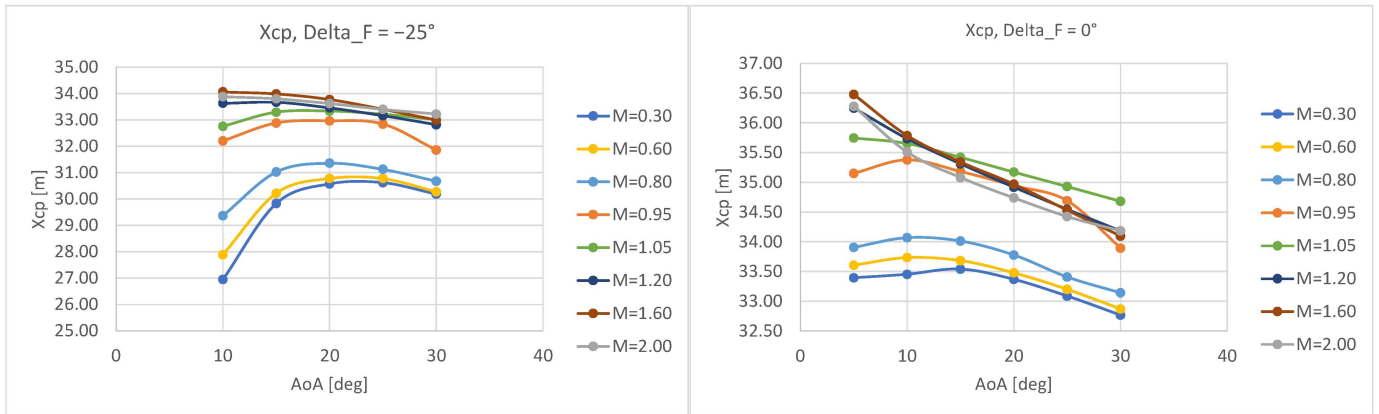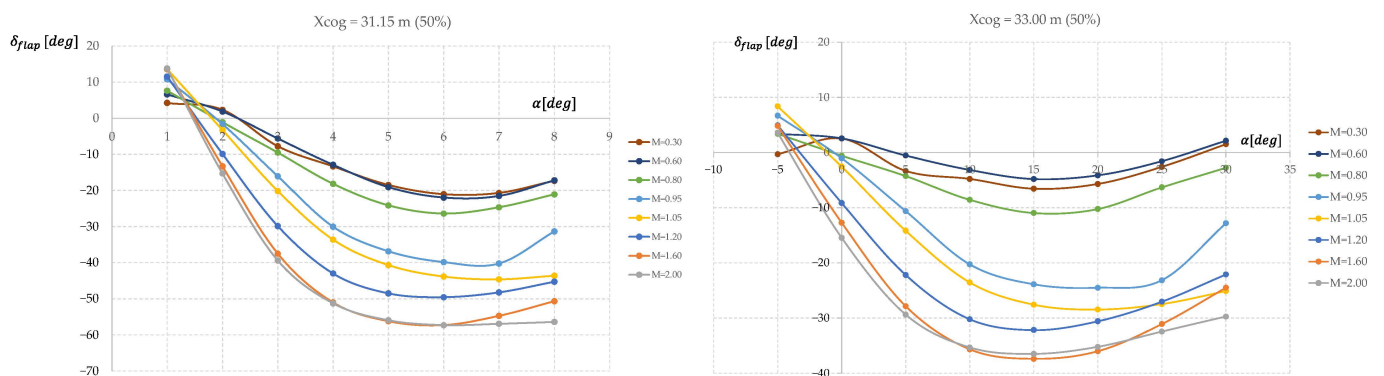

Figure 13. Centre of pressure behavior.

Figure 14. Deflection of control surfaces versus the angle of attack at each Mach number.
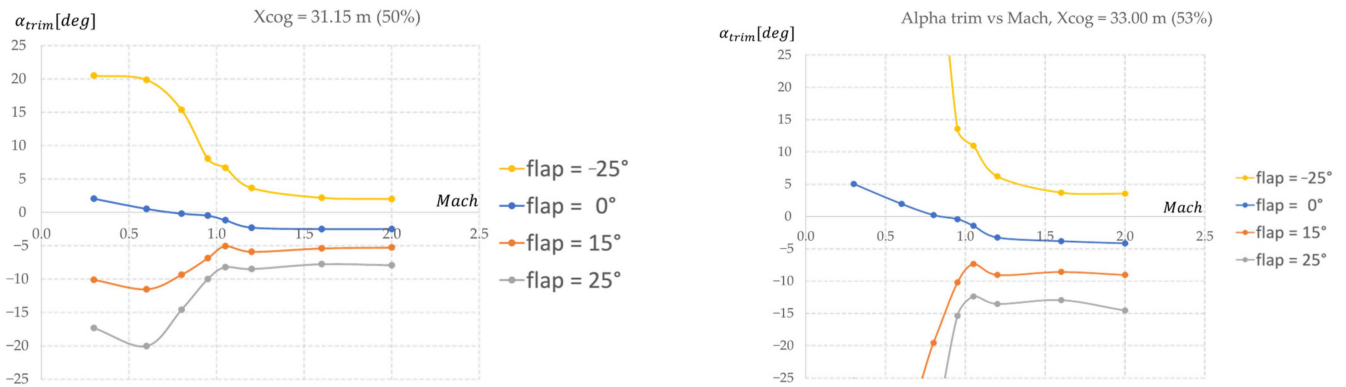
Figure 15. Angle of attack of trim versus the Mach number at a given flap deflection.

As a final check for the low-fidelity procedure, some viscous CFD simulations were performed at an angle of attack of zero degrees on a computational grid of nearly 13 million cells (Figure 16), with a layer of several prisms near the wall with a Delta_y at a wall of about 10^{-5} m that can guarantee a unit order of magnitude for the nondimensional distance from the wall y^+ ($y^+ = y/\delta_v$, $\delta_v = \nu/u_t$, $u_t = (\tau_w/\rho)^{0.5}$, where ν is the kinematic viscosity, τ_w is the friction at the wall, and ρ is the density) and, thus, a correct boundary layer resolution. Moreover, a k-ω SST turbulence model was used for eddy-viscosity treatment. As can be seen from Figure 17, where viscous results, inviscid results, and inviscid results with viscous correction are compared, a discrepancy can be found in the transonic region for the lift coefficient, while a quite good comparison of results for the drag one all along the Mach number is obtained. This makes the procedure conservative. For the progress of the activity, no correction of the viscous effect will be considered. In general, the differences can be managed as uncertainties bars. Note that, being at AoA = $0°$, there is no effect of viscosity on the lift coefficient.
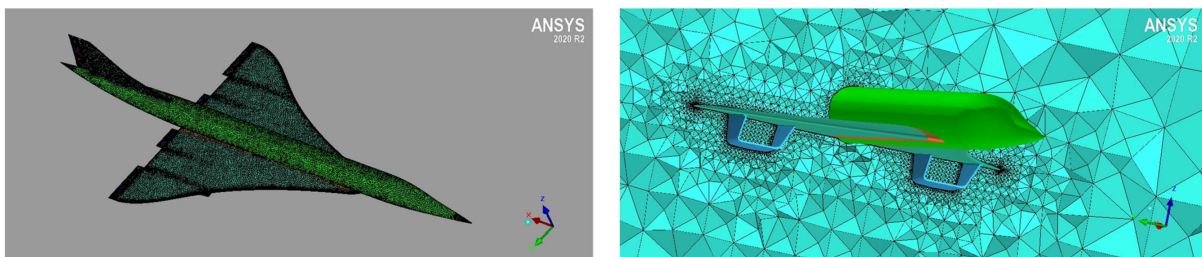

Figure 16. Grid of 13 M cells with boundary layer for viscous calculations.
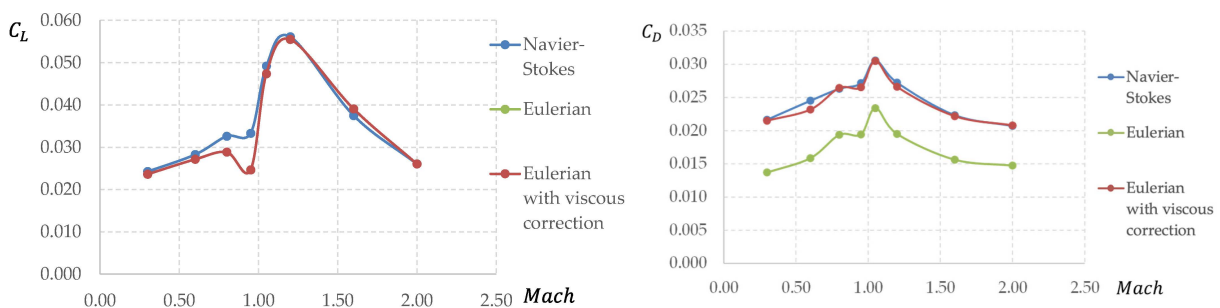

Figure 17. Effect of air viscosity on aerodynamic performance. Comparison between CFD NS and CFD EUL + viscous correction.

5. Trajectory Analysis

For this vehicle, an experimental test campaign is not foreseen, and so the reported results are the full aerodynamic activities that can feed the other disciplines as flight me-

chanics and structural analyses. In particular, a preliminary material-point flight mechanics analysis of the vehicle is possible in order to verify the feasibility of the mission in terms of flight time and fuel consumption. In this paper, the analysis of the propulsive database is not reported and we assume that the engines are always able to counteract all the forms of resistance such as the drag and the acceleration. In this way, we can consider the following work as an input for a propulsive system.

A comparison between two types of mission is reported: the clean one that is obtained for an undeflected aerodatabase that means no activation of control surfaces, and in this case, we are assuming the satisfaction of pitch control equilibrium; and the trimmed one, obtained considering a more realistic situation with the activation of the control surfaces. For the trim case, the center of gravity shifts from 33 m in the subsonic regime to a more backward position of 34.5 m for the supersonic regime.

From Figure 18, we can also observe the less regular trend of the angle of attack for the trim case if the average values are quite similar. The higher fuel consumption is directly linked to the lower values of aerodynamic efficiency (lift-to-drag ratio). In fact, the deflection of the control surfaces, for a position of the CoG ahead of the center of pressure (CoP), gives lower values of lift and higher values of drag. The amount of the variation of aerodynamic force coefficients depends on the distance between the abovementioned two points. In order to maintain the feasibility of the mission, the shift of CoG is necessary since the CoP shifts toward the tail as a consequence of the change in the flight regime from subsonic to supersonic (Figure 13). Another consequence is the reaching of a lower value of the altitude for the trim case. In any case, for a full flyability analysis, the accounting of the propulsive database is necessary.
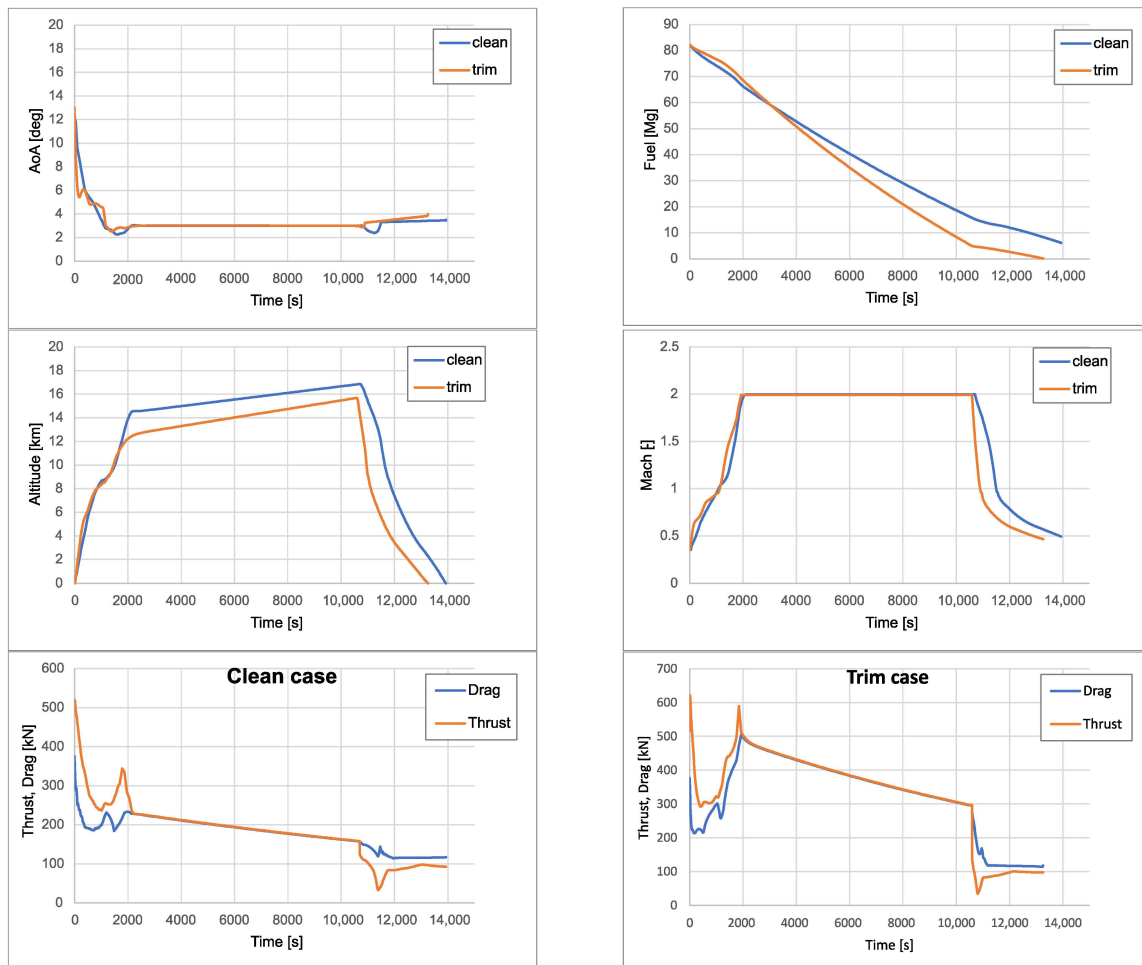

Figure 18. Preliminary trajectory calculations.

6. Conclusions

A whole procedure for the rapid and reliable development of a complete aerodynamic database and a first flyability analysis in terms of stability, trimmability, maneuverability, and fuel consumption for a civil supersonic configuration is reported here. This procedure is intended as a tool for a preliminary design phase of a generic supersonic/hypersonic civil aircraft with an increasing-fidelity aerodynamic modeling. A build-up approach is adopted that combines together the clean configuration, the control surfaces effects and, if any, the effect of the propulsion system. The reference configuration studied in this paper is the CS1 of the Horizon2020 MORE&LESS project, a Mach 2 supersonic cruiser similar to the Concorde. The preliminary trajectory analysis based only on the full aerodynamic database shows a flyable vehicle able to perform the given mission. Further calculations and inclusion of the propulsive database are necessary for a full mission feasibility analysis.

Author Contributions: Conceptualization, P.R., M.M. and R.F.; methodology, P.R., M.M., O.G., R.F. and N.V.; software, P.R. and O.G.; validation, P.R.; formal analysis, P.R. and M.M.; writing—original draft preparation, P.R. and O.G.; writing—review and editing, M.M., R.F. and N.V.; visualization, P.R.; supervision, M.M. and N.V.; project administration, M.M.; funding acquisition, N.V. All authors have read and agreed to the published version of the manuscript.

References

1. MDO and REgulations for Low-boom and Environmentally Sustainable Supersonic aviation. Available online: https://cordis.europa.eu/project/id/101006856 (accessed on 31 January 2022).
2. Viola, N.; Fusaro, R.; Ferretto, D.; Gori, O.; Saracoglu, B.; Ispir, A.C.; Schram, C.; Grewe, V.; Plezer, J.F.; Martinez, J.; et al. H2020 STRATOFLY Project: From Europe to Australia in less than 3 hours. In Proceedings of the 32nd Congress of the International Council of the Aeronautical Sciences, Shanghai, China, 6–10 September 2021.
3. Cariscia, S.A.; Locke, J.W.; Boyd, L.D.; Lewis, M.J.; Halion Sun, R.P.; Smith, H. *Commercial Development of Civilian Supersonic Aircraft*; IDA Coument D-10845; IDA Science and Technology Policy Institute: Washington, DC, USA, 2019.
4. Fusaro, R.; Ferretto, D.; Viola, N. Model-Based Object-Oriented systems engineering methodology for the conceptual design of a hypersonic transportation system. In Proceedings of the 2016 IEEE International Symposium on Systems Engineering (ISSE), Edinburgh, UK, 3–5 October 2016. [CrossRef]
5. Ferretto, D.; Fusaro, R.; Viola, N. A conceptual design tool to support high-speed vehicle design. In Proceedings of the AIAA Aviation 2020 Forum, Virtual, 15–19 June 2020. [CrossRef]
6. Cakir, B.O.; Ispir, A.C.; Saracoglu, B.H. Reduced order design and investigation of intakes for high speed propulsion systems. *Acta Astronaut.* **2022**, *199*, 259–276. [CrossRef]
7. Ispir, A.C.; Saracoglu, B.H.; Magin, T.; Coussement, A. A methodology for estimating hypersonic engine performance by coupling supersonic reactive flow simulations with machine learning techniques. *Aerosp. Sci. Technol.* **2023**, *140*, 108501. [CrossRef]
8. Goncalves, P.M.; Ispir, A.C.; Saracoglu, B.H. Development and optimization of a hypersonic civil aircraft propulsion plant with regenerator system. In Proceeding of the AIAA Propulsion and Energy 2019 Forum, Indianapolis, IN, USA, 19–22 August 2019. [CrossRef]
9. Steelant, J.; Varvill, R.; Walton, C.; Defoort, S.; Hannemann, K.; Marini, M. Achievements obtained for sustained hypersonic flight within the LAPCAT-II project. In Proceedings of the 20th AIAA International Space Planes and Hypersonic Systems and Technologies Conference, Glasgow, UK, 6–9 July 2015; p. 3677.
10. Fureby, C.; Nilsson, T. Large Eddy Simulation of cavity stabilized ramjet combustion. *Aerosp. Sci. Technol.* **2023**, *141*, 108503. [CrossRef]
11. Bonelli, F.; Cutrone, L.; Votta, R.; Viggiano, A.; Magi, V. Preliminary design of a hypersonic air-breathing vehicle. In Proceedings of the 17th AIAA International Space Planes and Hypersonic Systems and Technologies Conference, AIAA 2011-2319, San Francisco, CA, USA, 11–14 April 2011. [CrossRef]
12. Wood, R.M. *Supersonic Aerodynamics of Delta Wings*; NASA Technical Paper 2771; NASA: Houston, TX, USA, 1988.
13. Elle, B.J. *An Investigation at Low Speed of the Flow Near the Apex of Thin Delta Wing with Sharp Leading Edges*; Reports and Memoranda 3176; Aeronautical Research Council: London, UK, 1958.
14. Visbal, M.R. Onset of vortex breakdown above a pitching delta wing. *AIAA J.* **1994**, *32*, 1568–1575. [CrossRef]

15. Ekaterinaris, J.A.; Schiff, L.B. Numerical simulation of incidence and sweeep effects on delta wing vortex breakdown. *J. Aircr.* **1994**, *31*, 1043–1049. [CrossRef]
16. Gursul, I. Review of unsteady vortex flow over delta wings. *J. Aircr.* **2005**, *42*, 299–319. [CrossRef]
17. Taylor, G.; Gursul, I. Buffeting flows over a low sweep delta wing. *AIAA J.* **2004**, *42*, 1731–1745. [CrossRef]
18. Nelson, R.C.; Pelletier, A. The unsteady aerodynamics of slender wings and aircraft undergoing large amplitude maneuvers. *Prog. Aerosp. Sci.* **2003**, *39*, 185–248. [CrossRef]
19. Piccirillo, G.; Viola, N.; Fusaro, R.; Federico, L. Guidelines for the LTO Noise Assessment of Future Civil Supersonic Aircraft in Conceptual Design. *Aerospace* **2022**, *9*, 27. [CrossRef]
20. Graziani, S. Sonic boom CFD near-field analysis of a Mach 5 configuration. *Mater. Res. Proc.* **2023**, *33*, 83–90. [CrossRef]
21. Pletzer, J.F.; Hauglustaine, D.; Cohen, Y.; Jöckel, P.; Grewe, V. The Climate Impact of Hypersonic Transport. *EGUsphere* 2022. [CrossRef]
22. Pletzer, J.F.; Grewe, V. Sensitivities of atmospheric composition and climate to altitude and latitude of hypersonic aircraft emissions. *EGUsphere* 2023. [CrossRef]
23. Viola, N.; Fusaro, R.; Gori, O.; Marini, M.; Roncioni, P.; Saccone, G.; Bodmer, D. STRATOFLY MR3–how to reduce the environmental impact of high-speed transportation. In Proceedings of the AIAA Scitech 2021 Forum, Virtual, 11–15 & 19–21 January 2021; p. 1877.
24. Roncioni, P.; Vitagliano, P.L.; De Gregorio, F.; Pezzella, G.; Romano, L.; Paglia, F. Aerodynamic Appraisal of the VEGA-C Launcher. *J. Spacecr. Rocket.* **2023**, *60*, 5. [CrossRef]
25. Sun, Y.; Smith, H.; Chen, H. *Conceptual Design of Low-Boom Low-Drag Supersonic Transports*; American Institute of Aeronautics and Astronautics: Reston, VA, USA, 2020.
26. Aprovitola, A.; Di Nuzzo, P.E.; Pezzella, G.; Viviani, A. Aerodynamic Analysis of a Supersonic Transport Aircraft at Landing Speed Conditions. *Energies* **2021**, *14*, 6615. [CrossRef]
27. Aprovitola, A.; Dyblenko, O.; Pezzella, G.; Viviani, A. Aerodynamic Analysis of a Supersonic Transport Aircraft at Low and High Speed Flow Conditions. *Energies* **2022**, *9*, 411. [CrossRef]
28. Pamadi, B.N.; Brauckmann, G.J.; Ruth, M.J.; Fuhrmann, H.D. Aerodynamic Characteristics, Database Development and Flight Simulation of the X-34 Vehicle. In Proceedings of the 38th Aerospace Sciences Meeting & Exhibit, Reno, NV, USA, 10–13 January 2000. [CrossRef]
29. Fusaro, R.; Gori, O.; Ferretto, D.; Viola, N.; Roncioni, P.; Marini, M. Integration of an increasing fidelity aerodynamic modelling approach in the conceptual design of hypersonic cruiser. In Proceedings of the 32nd Congress of the International Council of the Aeronautical Sciences, Shanghai, China, 6–10 September 2021.
30. Viola, N.; Roncioni, P.; Gori, O.; Fusaro, R. Aerodynamic Characterization of Hypersonic Transportation Systems and Its Impact on Mission Analysis. *Energies* **2021**, *14*, 3590. [CrossRef]
31. Anderson, J.D. *Hypersonic and High Temperature Gas Dynamics*; McGraw-Hill: New York, NY, USA, 1989.
32. Anderson, J.D. *Fundamentals of Aerodynamics*, 5th ed.; McGraw-Hill: New York, NY, USA, 2011.
33. Raymer, D.P. *Aircraft Design: A Conceptual Approach*, 6th ed.; Schetz, J.A., Ed.; AIAA Education Series; AIAA: Reston, VA, USA, 2018. [CrossRef]
34. Schlichting, H. *Boundary Layer Theory*; McGraw-Hill: New York, NY, USA, 1979.
35. Roncioni, P.; Vitagliano, P.L.; De Gregorio, F.; Paglia, F.; Milana, C. Aerodatabase of Vega C Launcher Development and Integration. In Proceedings of the 8th European Conference for Aeronautics and Space Sciences (EUCASS), Madrid, Spain, 1–4 July 2019.
36. Langener, T.; Erb, S.; Steelant, J. Trajectory Simulation and Optimization of the LAPCAT MR2 Hypersonic Cruiser Concept. In Proceedings of the 29th Congress of the International Council of the Aeronautical Sciences, St. Petersburg, Russia, 7–12 September 2014. ICAS 2014 428.
37. Fusaro, R.; Ferretto, D.; Viola, N. MBSE approach to support and formalize mission alternatives generation and selection processes for hypersonic and suborbital transportation systems. In Proceedings of the 2017 IEEE International Systems Engineering Symposium (ISSE), Vienna, Austria, 11–13 October 2017. [CrossRef]